Journal of Plankton Research Vol.22 no.3 pp.409–420, 2000

3D spatial point patterns of bioluminescent plankton: a map of the 'minefield'

Edith A.Widder[1] and Sönke Johnsen

Marine Science Division, Harbor Branch Oceanographic Institution, Fort Pierce, FL 34946, USA

[1]*To whom correspondence should be addressed*

Abstract. As the open ocean environment lacks points of refuge from visual predators, it has favored the evolution of extraordinary adaptations for optical concealment, such as vertical migration, transparency and counterillumination. Bioluminescent plankton, which respond to a mechanical disturbance with a flash of light, are ubiquitous in the ocean and potentially a threat to any organism seeking darkness as a means to evade detection. Estimating encounter probabilities for organisms maneuvering through luminescent 'minefields' requires characterization of the three-dimensional distribution patterns of the potential light emitters. In order to measure nearest neighbor distances (NNDs) of bioluminescent biota, we have developed a spatial plankton analysis technique (SPLAT) for 3D reconstruction and statistical analysis of the spatial point patterns of identified bioluminescent displays. Analysis of aggregations of bioluminescent biota in the Gulf of Maine (Wilkinson Basin) revealed that encounter probabilities were highest in the temperature minimum zone (temperature <5°C) where dinoflagellates (*Protoperidineum depressum*) exhibited NNDs of 3.5–3.8 cm in a regular distribution pattern. This technique was also used to examine the internal organization of thin layers of the bioluminescent copepod, *Metridia lucens*. Comparison of night-time surface (migrating) and deep (non-migrating) layers indicated complete spatial randomness in both populations and no significant difference in spacing (NNDs: 9.5–13 cm).

Introduction

Light is a critical determinant of organism distributions and population dynamics in the marine environment. Characterizing the light field in the ocean has therefore become an important branch of oceanography. Although bioluminescence dominates the submarine light field at depths below the penetration of sunlight and at night in surface waters, the nature of this biological light field is not well known. While bioluminescence has been observed for centuries, it was not actually measured until the mid 1950s when researchers, using sensitive photomultiplier tubes to measure the penetration of daylight in the ocean, also recorded flashes of light at depths where sunlight was attenuated approximately eightfold (Clarke and Wertheim, 1956). After it became apparent that it was actually the movement of the light meter that was stimulating the bioluminescence, investigators began developing bathyphotometers designed to measure stimulated bioluminescence [e.g. (Clarke and Kelly, 1965; Seliger *et al*., 1969; Gitel'zon *et al*., 1973; Losee, *et al*., 1985; Swift *et al*., 1985; Widder *et al*., 1993)]. These instruments have furnished abundant evidence of the pervasiveness of bioluminescence in the oceans. Interestingly, despite the prevalence of potential bioluminescent sources in the water column, observations from submersibles suggest that, in the open ocean environment, bioluminescence is employed very conservatively (Widder *et al*. 1989, 1992; Widder and Johnsen, 1998). Even when a submersible underway is surrounded by so many flashing sources that the light falling on the

© Oxford University Press 2000

instruments and gauges appears as a continuous glow, once the sub is trimmed, so that there is no movement relative to the surrounding water mass, all flashing ceases (E.W., personal observation). Such an environment, where the slightest movement risks triggering an explosion of light, would appear to be a potential minefield for any organism trying to evade detection. Recent laboratory experiments demonstrating increased susceptibility of zooplankton to visual predators in the presence of bioluminescent dinoflagellates support this view (Mensinger and Case, 1992; Abrahams and Townsend, 1993; Fleisher and Case, 1995). In order to know how difficult it might be for an organism to avoid stimulating bioluminescence, it is necessary to characterize the three-dimensional distribution patterns of the potential light emitters. In the fluid environment of the open ocean such measurements are problematic compared with terrestrial or benthic environments where co-ordinates can be referenced to fixed landmarks. Also, since the size of luminescent sources range from microns (e.g. dinoflagellates) to meters (e.g. siphonophores), there exists the added demand of high resolution in a large field of view.

By using an intensified video camera mounted on a mid-water submersible it is possible to record bioluminescent displays that are mechanically stimulated to luminesce during horizontal transects. The unique temporal and spatial characteristics of these displays permit identification of many sources to the species level, and the exceptional signal-to-noise ratio afforded by a self-luminous source means that even microscopic organisms (e.g. a 50 μm dinoflagellate) can be identified in a field of view of 1 m (Widder *et al*., 1989, 1992; Widder, 1997). The analysis of these video data has recently been simplified with the development of a computer image recognition program that can identify bioluminescent displays based on their spatial and temporal characteristics (Widder and Johnsen, 1998; Widder *et al*., 1999). The resulting dataset, which is basically a set of points distributed in space, is known as a spatial point pattern. Although there are well established procedures for the statistical analysis of spatial point patterns (Diggle, 1983), these have generally been applied to two-dimensional datasets. Here, we describe a procedure for the statistical analysis of our three-dimensional datasets. Known as the spatial plankton analysis technique (SPLAT), this procedure not only provides a new perspective on the nature of the bioluminescence light field, it also provides information about the internal organization of plankton aggregations, about which very little is known.

The aggregations chosen for analysis were some on which we recently reported from the Gulf of Maine (Widder *et al*., 1999): (i) aggregations of the bioluminescent dinoflagellate *Protoperdinium depressum* found in the temperature minimum zone (temperature <5°C) and (ii) very thin layers (0.5 m) of the bioluminescent copepod *Metridia lucens*. Analysis of the dinoflagellate layers was undertaken to determine the encounter probabilities for organisms maneuvering through the highest densities of bioluminescent biota in the water column. Analysis of the copepod layers was undertaken in order to determine whether the spacing of individuals within these very thin layers was suggestive of a behavioral aggregation where interaction between individuals would require that the nearest neighbor distances (NNDs) be within what might be considered a reasonable

perceptive distance for a copepod [≤13 mm (Haury and Yamazaki, 1995)], or whether they were more likely to be aggregating at the locus of some resource or environmentally favorable state. Also, because *M.lucens* is a strong vertical migrator that characteristically demonstrates bimodal night-time distribution patterns, with adult females located primarily in surface layers and adult males remaining primarily at depth (Bollens *et al*. 1993; Osgood and Frost, 1994), an analysis of deep versus shallow layers provided an exceptional opportunity to look for differences in the internal organization of these two populations.

Method

A series of *Johnson-Sea-Link* submersible dives was made during a research cruise in the Gulf of Maine (Wilkinson Basin 42°N: 69°W) in August 1992. Video recordings of stimulated bioluminescence were made with an intensified video camera (ISIT 66, Dage-MTI, Michigan City, IN, USA) mounted inside the observation sphere of the submersible. A 1 m diameter flat transect screen with 1800 μm mesh NITEX® nylon stretched across it was secured in front of the sphere. Video recordings were made of bioluminescence that was mechanically stimulated as organisms bumped into, or passed through the screen during horizontal transects run at a forward speed of 0.3 m s^{-1}. Simultaneous with each transect a quantitative plankton sample was collected by a suction sampling pump with an in-line flow meter and a 64 μm mesh screen at the outflow to the collection buckets. As has been described previously, the organisms responsible for the bioluminescence recorded in each transect were identified based on the spatial and temporal properties of the recorded displays, and identifications were confirmed by correlation with the abundance of identified bioluminescent organisms in the quantitative plankton samples (Widder, 1997; Widder *et al*., 1999). The 3D spatial distributions of identified displays were then analyzed using an object-oriented image analysis routine. Video frames were digitized and then set to threshold and smoothed to remove camera noise. After this processing, each video frame consisted of white shapes (representing the instantaneous bioluminescent displays and referred to as 'slices') on a black background. The slices were combined with contiguous slices on subsequent video frames to construct objects (representing the complete bioluminescent events and referred to as 'blobs'). Blobs were then classified based on length (number of frames where blob is visible), volume (number of pixels in blob) and maximum area (number of pixels in largest slice of blob). The classified blobs, as well as the x and y values and the frame number (converted to z value based on the forward speed of the submersible) of the initial impact point, were then used for 3D reconstruction and statistical analysis of the original transect volume. In order to avoid possible edge effects, the image analysis was confined to a rectangular region of interest (ROI) at the center of the transect screen. The point of origin for each transect volume was the upper left hand corner for this ROI starting with Frame no. 1, which was selected as a point in time at least 20 s after the start of the transect.

Known as the Spatial Plankton Analysis Technique (SPLAT), the statistical analysis used Monte Carlo simulations to create random distributions of blobs of

a given type (copepod or dinoflagellate) within a transect volume. Although the statistical properties of NNDs in three dimensions are known (Rothschild, 1992), in this case, the considerable complications due to edge effects and the finite size of the bioluminescent events suggest the use of Monte Carlo methods. A cumulative histogram of nearest neighbor distances resulting from 5000 simulations (1000 in the case of the dinoflagellate layers) was plotted and used as a model of complete spatial randomness and then compared with the cumulative histograms of nearest neighbor distances calculated from the output of the blob classification program. An example of such an analysis is shown in Figure 1, which, for illustration purposes, uses two-dimensional rather than three-dimensional spatial point patterns. The location of each point in a dataset is referred to as an event. The *y*-axis indicates the proportion of events in a given data set with a nearest neighbor distance equal to, or less than the value indicated on the *x*-axis. Each histogram contains four plots: the average of 100 simulations (dotted line), the upper and lower envelopes (dashed lines), and the data (solid line). The upper and lower envelopes show the highest and lowest values achieved by any simulation for a given nearest neighbor distance. Figure 1a shows a regular distribution pattern. The cumulative histogram of the data shows that there is a distinct lack of small nearest neighbor distances. While the Monte Carlo simulations indicated that a completely random spatial distribution would predict that ~84% of the events should have NNDs of 8 cm or less, the actual dataset indicated a much smaller proportion of 21%. With 100 simulations, the smallest fraction of the population that resulted in NNDs less than or equal to 8 cm was 72%, indicating that the actual data are well outside the envelope of what could be accounted for by chance alone. Figure 1b shows a random pattern. The cumulative histogram is not significantly different from the average of the simulations. Figure 1c shows an aggregated or clumped pattern. The cumulative histogram shows that there is a significant surplus of small nearest neighbor distances. *P*-values were calculated using a U^2 statistic. This statistic is the sum of the squares of the deviations from the average cumulative histogram and was calculated for the data and all the simulations. The rank of the U^2 value of the data relative to the values of the simulations was used to determine the *P*-value (the probability that the NND of the data is due to chance) [see (Diggle, 1983) for a complete discussion of the analysis of spatial point patterns using Monte Carlo methods].

Since the bioluminescent signatures of the actual data were not points but had finite extent, the Monte Carlo simulations also used objects of finite extent. The shape and size of each simulated bioluminescent event was chosen from a distribution created from actual events. This added refinement is necessary to avoid a false determination of a regular distribution due to a mismatch between the sizes of the real bioluminescent events and the simulated events.

All software was written using Visual C++ (version 4.0 Microsoft Inc., Redmond, WA, USA) and run on a Dell 200 PC clone with a Pentium processor (Dell Computer Corporation, Round Rock, TX, USA). As mentioned above, only 1000 simulations were done for the dinoflagellate layers. This is due to the fact that CPU time for the simulations was proportional to the square of the number of animals. Since the number of dinoflagellates was ~35 times the number

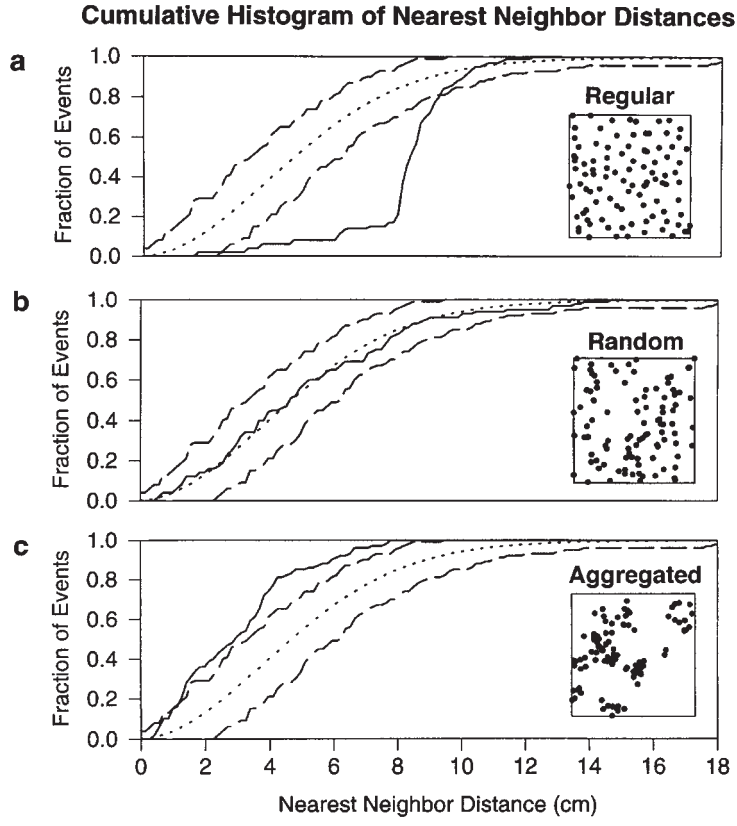

Fig. 1. Examples of regular (**a**), random (**b**) and aggregated (**c**) distributions with their associated cumulative histograms superimposed on the cumulative histograms generated by 100 Monte Carlo simulations. The dotted line shows the average of the simulations. The dashed lines show the upper and lower envelopes. The solid line shows the data.

of copepods, CPU time for 5000 simulations of the dinoflagellate layers was prohibitive.

Results

3D reconstruction of dinoflagellate and copepod layers

Figure 2 shows the 3D reconstruction of displays recorded in three of the layers selected for statistical analysis. Figure 2a shows displays recorded in a dinoflagellate layer during a transect made on Aug 17 at 61 m. Figure 2b shows displays recorded in a shallow (migrating) copepod layer on August 17 at 31 m. Figure 2c shows displays recorded in a deep (non-migrating) copepod layer on August 17 at 160 m. As described in Widder *et al.* (Widder *et al.*, 1999), the small clouds of bioluminescence shown in blue were characteristic of the bioluminescent copepod *Metridia lucens*, while the short duration, intrinsic displays shown

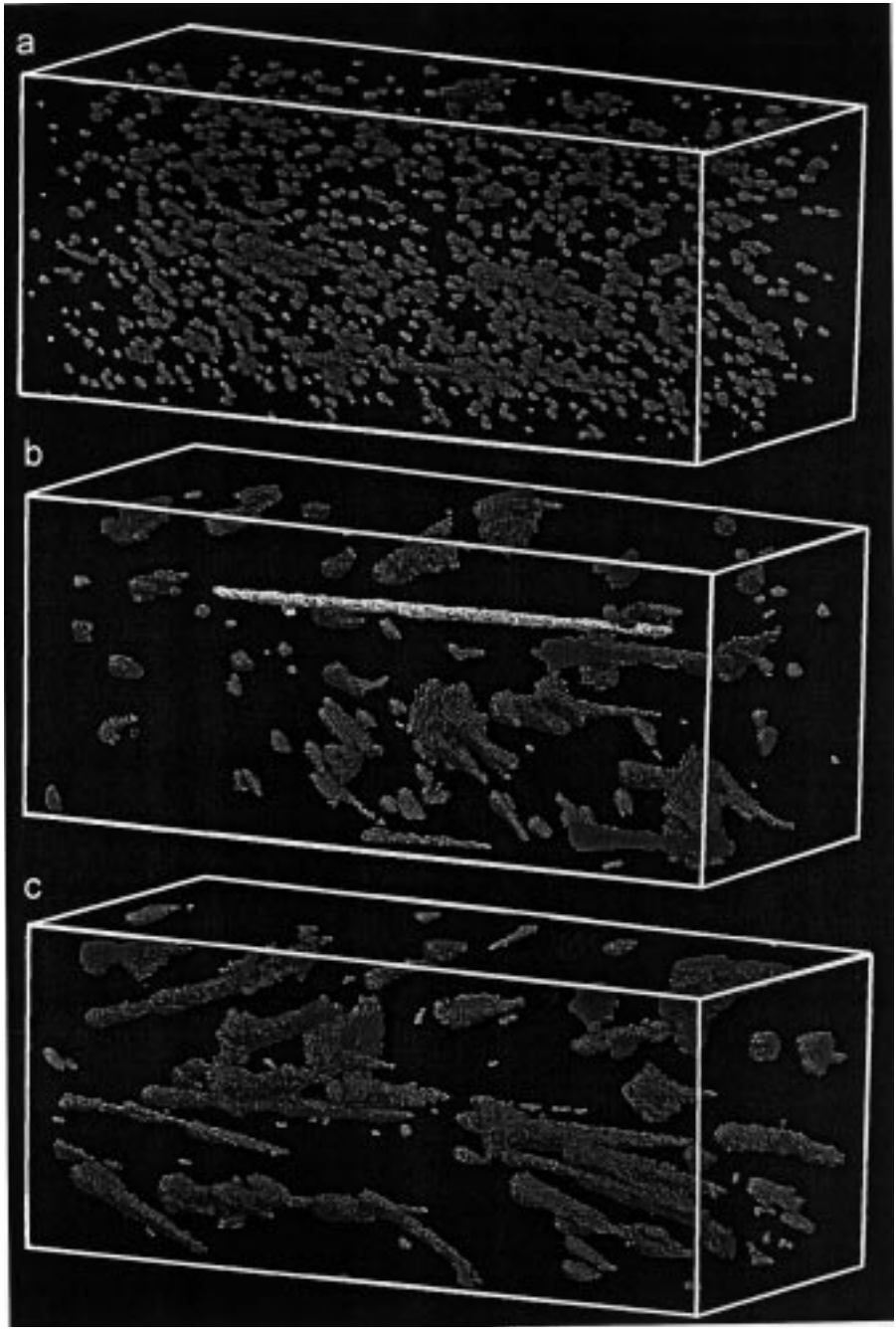

Fig. 2. 3D reconstruction of displays recorded in three of the layers selected for statistical analysis. Dinoflagellates are indicated in green, copepods in blue and euphausiids in yellow. (**a**) Displays recorded in a dinoflagellate layer during a transect made on Aug 17 at 61 m. (**b**) Displays recorded in a shallow (migrating) copepod layer on August 17 at 31 m. (**c**) Displays recorded in a deep (non-migrating) copepod layer on August 17 at 160 m. Each wire frame represents $0.35 \times 0.35 \times 3.0$ m.

in green were characteristic of the bioluminescent dinoflagellate *Protoperdinium depressum*. The persistent glow shown as yellow in Figure 2b is characteristic of the euphausiid *Meganyctiphanes norvegica*.

Nearest neighbor analyses of dinoflagellate layers

Table I shows the results of the nearest neighbor analyses for two dinoflagellate layers. The densities of bioluminescent biota within the two layers were 3228 and 3841 biota m^{-3}. The median nearest neighbor distances were 3.8 and 3.5 cm, and the exclusion distances (distances below which <1% of the nearest neighbors were found) were both 1.4 cm. The layers with the higher densities had the lower median nearest neighbor distance. Figure 3 shows the cumulative nearest neighbor histograms of the two layers superimposed on the results of 1000 Monte Carlo simulations. In both cases there is a significant lack of small nearest neighbor distances, indicating a regular pattern. The U^2 values for both layers are higher than the values for all 1000 simulations, showing a significant departure from complete spatial randomness.

Nearest neighbor analyses of night-time shallow and deep copepod layers

Table II shows the results of the nearest neighbor analyses for four copepod layers, two shallow and two deep. The copepod densities within the layers ranged from 103 to 229 animals m^{-3}. The median nearest neighbor distances ranged from 9.5 to 13 cm, and the exclusion distances ranged from 3.1 to 4.7 cm. Layers with higher copepod densities had lower median nearest neighbor distances and higher exclusion distances. Figure 4 shows the cumulative nearest neighbor histograms of the four layers superimposed on the results of 5000 Monte Carlo simulations. Except for a minor lack of small nearest neighbor distances at 16 m on August 18, all four cumulative histograms fall well within the envelopes of the simulations over their whole extent. The ranks of the U^2 statistic of the four layers all show no significant deviation from complete spatial randomness.

Discussion

The densest packing of bioluminescent biota that we found during this period in Wilkinson Basin was in the temperature minimum zone (temperature <5°C)

Table I. Results of statistical analysis of spatial point patterns in dinoflagellate layers

Transect date and depth	Density[a]	Exclusion distance[b]	Median nearest neighbor distance	U^2 statistic rank
August 17 Depth 61 m	3228	1.4 cm	3.8 cm	>all 1000 simulations
August 20 Depth 98 m	3841	1.4 cm	3.5 cm	>all 1000 simulations

[a]Bioluminescent events per cubic meter.
[b]Distance below which <1% of nearest neighbors were found.

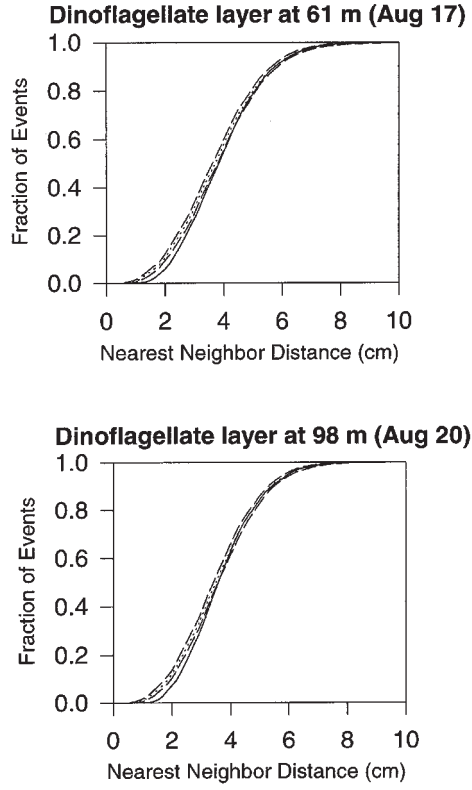

Fig. 3. Cumulative histograms for the two dinoflagellate layers superimposed on the cumulative histograms generated by 1000 Monte Carlo simulations. Lines are as described in Figure 1.

Table II. Results of statistical analysis of spatial point patterns in copepod layers

Transect date and depth	Density[a]	Exclusion distance[b]	Median nearest neighbor distance	U^2 statistic rank
August 17 Depth 31 m	103	3.1 cm	13 cm	>796 of 5000 simulations
August 17 Depth 160 m	140	4.5 cm	11 cm	>3091 of 5000 simulations
August 18 Depth 16 m	229	4.7 cm	9.5 cm	>4628 of 5000 simulations
August 18 Depth 155 m	159	3.9 cm	11 cm	>4358 of 5000 simulations

[a]Bioluminescent events per cubic meter.
[b]Distance below which <1% of nearest neighbors were found.

where the dominant luminescent source was the dinoflagellate *Protoperidinium depressum* (Widder *et al*., 1999). The luminescent minefield that organisms must negotiate in this zone had median nearest neighbor distances of 3.5–3.8 cm. Also in this layer, we found a deficiency of small nearest neighbor distances, a pattern

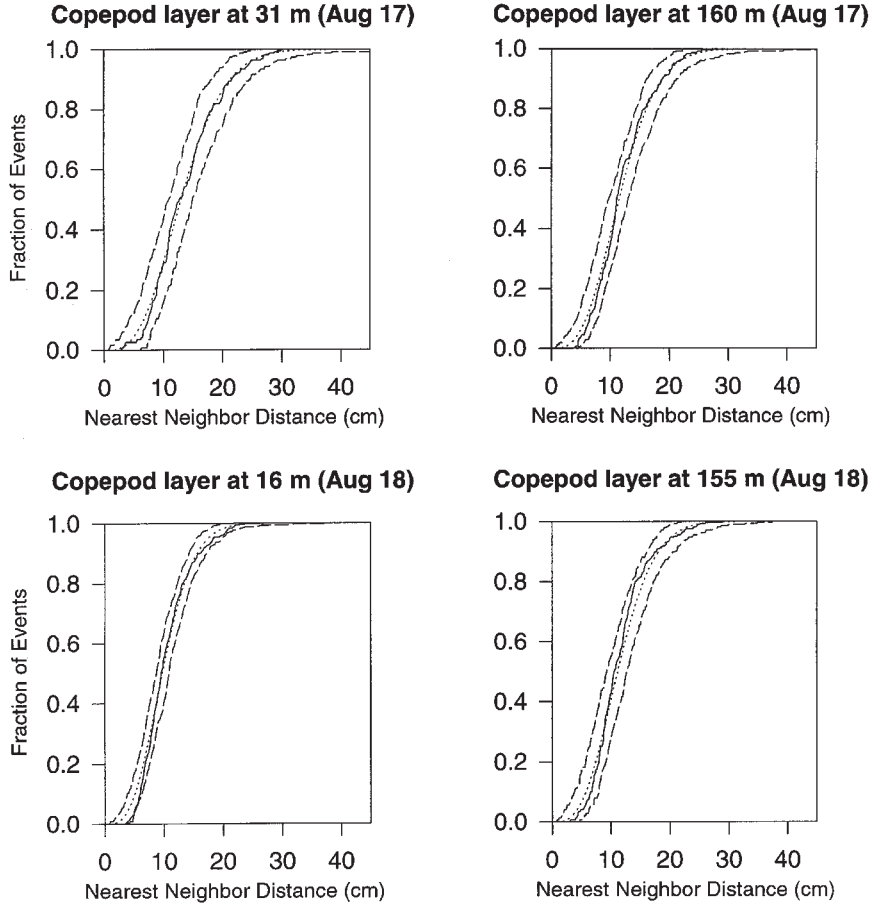

Fig. 4. Cumulative histograms for the four copepod layers superimposed on the cumulative histograms generated by 5000 Monte Carlo simulations. Lines are as described in Figure 1.

which is characterized as 'regular' (Diggle, 1983). At low abundances it is not possible to distinguish this pattern from random chance. However, where *P.depressum* was found in abundances of >3200 m^{-3}, there was a statistically significant difference in the nearest neighbor distances from that predicted by complete spatial randomness (CSR) (U^2 test, $P < 0.001$).

Dinoflagellates exist in a low Reynolds number fluid regime ($R_e < 0.025$) where a swimming cell disturbs flow at hundreds of diameters from the outer surface of the cell (Vogel, 1981; Levandowsky and Kaneta, 1987). From our nearest neighbor distance analysis, the zone of exclusion (the distance below which <1% of the nearest neighbors are found) for *P.depressum* was ~1.5 cm or 150 diameters for a 100 μm diameter cell. Dinoflagellates exhibit avoidance reactions in response to mechanical stimuli and alter their swimming direction in response to low

intensity stimuli (Levandowsky and Kaneta, 1987). Therefore, regularity might be viewed as a predictable pattern for microscopic, reactive organisms swimming in a fluid medium. This is, however, the first report of such a pattern *in situ* and has significant ramifications in understanding how the spacing of microscopic organisms in a fluid environment impacts resource utilization, dispersion and encounter probabilities between consumers and prey.

The range of nearest neighbor distances found for copepods in the thin layers (9.5–13 cm) indicated that these aggregations were not likely to be the consequence of purely behavioral interactions but were more likely due to orientation to some cue, such as a food source, or some environmentally favorable condition, such as a region of reduced current shear [see (Widder *et al*., 1999) for further discussion of this point]. The reasoning behind this hypothesis is that the distance between individuals was nearly 10 times greater than the maximum reported perceptive distance of a copepod (Haury and Yamazaki, 1995). However, recent evidence that male copepods can detect and follow a trail left by a swimming female for distances of more than 13 cm suggests that previously reported perceptive distances may not accurately reflect the true sensory range of an individual (Doall *et al.*, 1998). Although a large median NND cannot be used as evidence that *M.lucens* was not detecting and reacting to the presence of conspecifics, the lack of any evidence of clumping (i.e. an abundance of small NNDs) within the layers makes the behavioral explanation less probable. In fact, comparison of nearest neighbor distances for *M.lucens* with the Monte Carlo simulations indicated that these data were compatible with a completely random spatial distribution of these sources within the layers. This was the case in both shallow and deep layers, indicating no apparent difference in the internal organization of the migrating and non-migrating populations of *M.lucens*.

Unobtrusive sampling of animal distribution patterns in the ocean is greatly complicated by the presence of so much luminescence. Any sampling system moving through the water will stimulate bioluminescence, thereby alerting visual organisms of its approach. In the present study, although *M.lucens* lacks an image-forming eye, it does exhibit a startle response to flashes of light. The possible impact of this behavior on the spatial point patterns we recorded will depend on the threshold stimulus required and the length of the swimming burst it elicits. *Metridia lucens* exposed to flashes of artificial light of 1.2×10^{14} photons cm^{-2} s^{-1} approximately doubled their average swimming speeds from 4 to 8.5 mm s^{-1} with no apparent preferred direction relative to the stimulus (Buskey and Swift, 1985). If we assume a threshold sensitivity comparable with that demonstrated in the copepod *Pleuromamma xiphias* of 7×10^7 photons cm^{-2} s^{-1} (Buskey *et al*., 1989), then *M.lucens* could detect the screen as much as 3 s before contact and therefore may have moved as much as 2.6 cm. The possible impact of this effect on spatial point patterns will be addressed in the future by running transects at different speeds.

Light and life in the sea are intimately linked. Characterizing the submarine light field and how it influences plankton populations has therefore become a critical aspect of understanding ecological processes in the ocean. The spatial plankton analysis technique described here provides a new perspective on the

optical complexity of the submarine light field, as well as revealing new information about the internal organization of bioluminescent aggregations.

Acknowledgements

We thank T.Frank, S.Bernstein, S.Haddock, R.Beard, K.Eichenhorst, the captain and crew of the RV 'Seward Johnson' and the pilots and crew of the 'Johnson-Sea-Link' submersible for assistance at sea, and K.Christensen and D.Smith for assistance with computer image analysis. Supported by ONR grant N0001490J1819, NOAA/NURP grant UCAP9221 and NSF grant OCE9318399 (E.A.W.), HBI postdoctoral fellowship (S.J.). Contribution no. 1330 of Harbor Branch.

References

Abrahams,M.V. and Townsend,L.D. (1993) Bioluminescence in dinoflagellates: a test of the burglar alarm hypothesis. *Ecology*, **74**, 258–260.

Bollens,S.M., Osgood,K.E., Frost,B.W. and Watts,S.D. (1993) Vertical distributions and susceptibilities to vertebrate predation of the marine copepods *Metridia lucens* and *Calanus pacificus*. *Limnol. Oceanogr.*, **38**, 1827–1837.

Buskey,E.J. and Swift,E. (1985) Behavioral responses of oceanic zooplankton to simulated bioluminescence. *Biol. Bull.*, **168**, 263–275.

Buskey,E.J., Baker,K.S., Smith,R.C. and Swift,E. (1989) Photosensitvity of the oceanic copepods *Pleuromamma gracilis* and *Pleuromamma xiphias* and its relationship to light penetration and daytime depth distribution. *Mar. Ecol. Prog. Ser.*, **55**, 207–216.

Clarke,G.L. and Kelly,M.G. (1965) Measurements of diurnal changes in bioluminescence from the sea surface to 2000 meters using a new photometric device. *Limnol. Oceanogr.*, **10**, R54–R66.

Clarke,G.L. and Wertheim,G.K. (1956) Measurements of illumination at great depths and at night in the Atlantic Ocean by means of a new bathyphotometer. *Deep-Sea Res.*, **4**, 189–205.

Diggle,P.J. (1983) *Statistical Analysis of Spatial Point Patterns.* Academic Press, London.

Doall,M.H., Colin,S.P., Strickler,J.R. and Yen,J. (1998) Locating a mate in 3D: the case of *Temora longicornis*. *Phil. Trans. R. Soc. Lond. B*, **353**, 681–1689.

Fleisher,K. and Case,J.F. (1995) Enhancement of cephalopod predation by dinoflagellate luminescence. *Biol. Bull.*, **189**, 263–271.

Gitel'zon,I.I., Levin,L.A., Shevyrnogov,A.P., Utyushev,R.N. and Artemkin,A.S. (1973) Pelagic bathymetric sounding and its possible application to studies of the spatial structure of biocenoses. In Vinogradov,M.E. (ed.) *Life Activity of Pelagic Communities in the Ocean Tropics* (translated from Russian, Israel Program for Scientific Translations). Israel Program for Scientific Translations, Jerusalem, pp. 51–66.

Haury,L.R. and Yamazaki,H. (1995) The dichotomy of scales in the perception and aggregation behavior of zooplankton. *J. Plankton Res.*, **17**, 191–197.

Levandowsky,M. and Kaneta,P.J. (1987) Behaviour in dinoflagellates. In Taylor,F.J.R. (ed.) *The Biology of Dinoflagellates.* Blackwell Scientific Publications, Oxford, pp. 360–397.

Losee,J., Lapota,D. and Lieberman,S.H. (1985) Bioluminescence: a new tool for oceanography. In Zirino,A. (ed.) *Mapping Strategies in Chemical Oceanography.* American Chemical Society, Vol. 209, pp. 211–234.

Mensinger,A.F. and Case,J.F. (1992) Dinoflagellate luminescence increases susceptibility of zooplankton to teleost predation. *Mar. Biol.*, **112**, 207–210.

Osgood,K.E. and Frost,B.W. (1994) Ontogenetic diel vertical migration behaviors of the marine planktonic copepods *Calanus pacificus* and *Metridia lucens*. *Mar. Ecol. Prog. Ser.*, **104**, 13–25.

Rothschild,B.J. (1992) Application of stochastic geomtery to problems in plankton ecology. *Phil. Trans. R. Soc. Lond. B*, **336**, 225–237.

Seliger,H.H., Fastie,W.G. and McElroy,W.D. (1969) Towable photometer for rapid area mapping of concentrations of bioluminescent marine dinoflagellates. *Limnol. Oceanogr.*, **14**, 806–813.

Swift,E., Biggley,W.H. and Lessard,L.J. (1985) Distributions of epipelagic bioluminescence in the Sargasso and Caribbean Seas. Advances in Chemistry Series #209: *Mapping Strategies in Chemical Oceanography.* American Chemical Society.

Vogel,S. (1981) *Life in Moving Fluids.* Princeton University Press, Princeton.
Widder,E.A. (1997) *In situ* video recordings of bioluminescence in the ostracod, *Conchoecia elegans,* and co-occuring bioluminescent zooplankton in the Gulf of Maine. In Hastings,J.W., Kricka,L.J. and Stanley,P.E. (eds) *Proceedings of the 9th International Symposium on Bioluminescence and Chemiluminescence*. John Wiley & Sons Ltd., New York, pp. 159–164.
Widder,E.A. and Johnsen,S. (1998) Optical imaging, identification and 3D analysis of spatial distribution patterns of bioluminescent plankton. SPIE Ocean Optics XIV (CD-ROM, File No. 1170ew.pdf).
Widder,E.A., Bernstein,S.A., Bracher,D.F., Case,J.F., Reisenbichler,K.R., Torres,J.J. and Robison,B.H. (1989) Bioluminescence in Monterey Submarine Canyon: image analysis of video recordings from a midwater submersible. *Mar. Biol.*, **100**, 541–551.
Widder,E.A., Greene,C.H. and Youngbluth,M.J. (1992) Bioluminescence of sound-scattering layers in the Gulf of Maine. *J. Plankton Res.*, **14**, 1607–1624.
Widder,E.A., Case,J.F., Bernstein,S.A., MacIntyre,S., Lowenstine,M.R., Bowlby,M.R. and Cook,D.P. (1993) A new large volume bioluminescence bathyphotometer with defined turbulence excitation. *Deep-Sea Res.*, **40**, 607–627.
Widder,E.A., Johnsen,S., Bernstein,S.A., Case,J.F. and Neilson,D.J. (1999) Thin layers of bioluminescent copepods found at density discontinuities in the water column. *Mar. Biol.*, **134**, 429–437.

Received on March 6, 1999; accepted on September 1, 1999